Trimethylsilyl-Substituted Hydroxycyclopentadienyl Ruthenium Hydrides as Benchmarks to Probe Ligand and Metal Effects on the Reactivity of Shvo Type Complexes

Charles P. Casey* and Hairong Guan

Department of Chemistry, University of Wisconsin-Madison,

Madison, Wisconsin 53706

casey@chem.wisc.edu

Supporting Information

Table of Contents

{2,5-(SiMe$_3$)$_2$-3,4-[(CH$_2$)$_4$](η^4-C$_4$CO)}Ru(CO)$_3$ (17). Method A: Under a nitrogen atmosphere, the cyclopentadienone ligand 2,5-(SiMe$_3$)$_2$-3,4-[(CH$_2$)$_4$](C$_4$CO) (314 mg, 1.13 mmol) and Ru$_3$(CO)$_{12}$ (230 mg, 0.36 mmol) were dissolved in 20 mL of degassed methanol. The resulting orange solution was heated at reflux under nitrogen for 2 days, at which point, the color of the solution turned to black. After cooling, the reaction mixture was concentrated under vacuum and the residue was subjected to column chromatography (eluted with 1/1 hexanes/CH$_2$Cl$_2$, and then with 1/1 hexanes/EtOAc). **17** was isolated as colorless crystals (250 mg, 48% yield).

Method B: The dialkyne Me$_3$SiC≡C(CH$_2$)$_4$C≡CSiMe$_3$ (5.26 g, 21 mmol), Ru$_3$(CO)$_{12}$ (3.84 g, 6 mmol), and glyme (15 mL) were mixed in a Fisher-Porter glass tube. The reaction vessel was charged with 5 atm CO pressure and sealed. The closed system was heated in a 140−150 ºC oil bath for 15 h. After cooling, the pressure was released and the reaction mixture was concentrated under vacuum. The crude product was purified by column chromatography using the same conditions as Method A to give **17** (4.81 g, 49% yield). ^{1}H NMR (CDCl$_3$, 300 MHz) δ 0.27 (s, Si(C*H*$_3$)$_3$, 18H), 1.76-1.84 (m, C*H*$_2$, 4H), 2.52-2.75 (m, C*H*$_2$, 4H). ^{13}C{^{1}H} NMR (CDCl$_3$, 126 MHz) δ 0.37 (Si(*C*H$_3$)$_3$), 22.82 (*C*H$_2$), 25.20 (*C*H$_2$), 68.90, 112.85, 184.79 (*C*=O), 195.31 (Ru(*C*O)$_3$). IR (CH$_2$Cl$_2$, cm^{-1}) 2076, 2016, 1999, 1614. HRMS (ESI) calcd (found) for [C$_{18}$H$_{26}$O$_4$Si$_2$Ru+H]$^{+\bullet}$ 465.0491 (465.0490).

[2,5-(SiMe$_3$)$_2$-3,4-[(CH$_2$)$_4$](η^5-C$_4$COH)]Ru(CO)$_2$H (18) was prepared in 88% yield by a procedure similar to that used for **10**. The isolated product always contained about 6 mol% of an impurity that was attributed to a diruthenium bridging hydride (δ -17.89 in benzene-*d*$_6$). ^{1}H NMR of **18** (benzene-*d*$_6$, 300 MHz) δ -9.92 (s, Ru*H*, 1H), 0.28 (s, Si(C*H*$_3$)$_3$, 18H), 1.20-1.27 (m, C*H*$_2$, 2H), 1.37-1.43 (m, C*H*$_2$, 2H), 2.05-2.14 (m, C*H*$_2$, 2H), 2.41-2.51 (m, C*H*$_2$, 2H), 3.89 (br s, O*H*, 1H). ^{13}C{^{1}H} NMR (benzene-*d*$_6$, 90 MHz) δ 1.64 (Si(*C*H$_3$)$_3$), 23.60 (*C*H$_2$), 25.94 (*C*H$_2$), 74.27, 107.74, 150.16 (*C*OH), 202.95 (Ru(*C*O)$_2$). IR (toluene, cm^{-1}) 2010, 1949.

[2,5-(SiMe$_3$)$_2$-3,4-(CH$_2$OCH$_2$)(η^5-C$_4$COH)]Fe(CO)$_2$H (16) was prepared from [2,5-(SiMe$_3$)$_2$-3,4-(CH$_2$OCH$_2$)(η^4-C$_4$CO)]Fe(CO)$_3$ in 57 % yield by a procedure similar to that used for **10**. ^{1}H NMR (benzene-*d*$_6$, 300 MHz) δ −11.65 (s, Fe*H*, 1H), 0.18 (s, Si(C*H*$_3$)$_3$, 18H), 3.64 (br s, O*H*, 1H), 4.20 and 4.50 (AB, J_{AB} = 9.9 Hz, C*H*$_2$, 4H). ^{13}C{^{1}H} NMR (benzene-*d*$_6$, 90 MHz) δ 0.29 (Si(*C*H$_3$)$_3$), 67.70, 68.16 (*C*H$_2$), 107.19, 147.19 (*C*OH), 216.02 (Fe(*C*O)$_2$). IR (toluene, cm^{-1}) 2007, 1950.

Table S1. Rate of reduction of PhCHO by ruthenium hydride **10** in toluene-d_8 at −53.5 ºC.

[**10**]$_0$ (M)	[PhCHO]$_0$ (M)	k_{obsd} (s^{-1}) [a]
0.0090	0.091	$2.6(1) \times 10^{-3}$
0.0084	0.145	$3.5(2) \times 10^{-3}$
0.0080	0.18	$4.0(3) \times 10^{-3}$
0.0076	0.22	$4.6(2) \times 10^{-3}$

[a] Average of three runs.

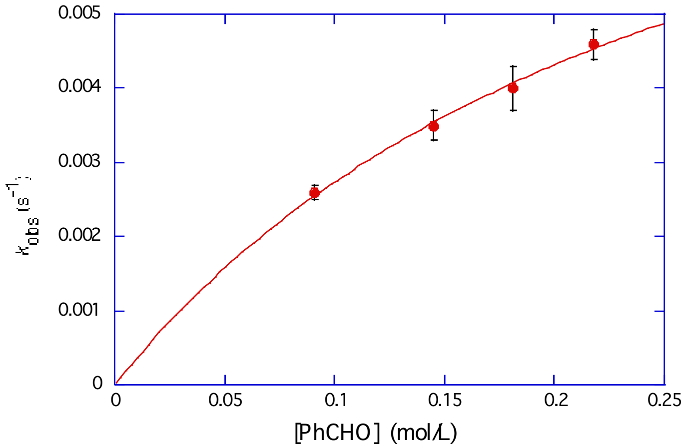

Figure S1. Plot of k_{obs} as a function of [PhCHO] in toluene-d_8 at −53.5 ºC.

$$\Rightarrow K_{eq} = 3.6 \pm 0.6\ M^{-1} \text{ and } k_2 = 1.0 \pm 0.1 \times 10^{-2}\ s^{-1}$$

Table S2. Rate of reduction of PhCHO by ruthenium hydride **10** in toluene-d_8 at -60.0 ºC.[a]

[**10**]$_0$ (M)	[PhCHO]$_0$ (M)	k_{obsd} (s^{-1}) [b]
0.0090	0.091	$1.41(5) \times 10^{-3}$
0.0084	0.145	$1.71(10) \times 10^{-3}$
0.0080	0.18	$1.91(14) \times 10^{-3}$
0.0076	0.22	$2.05(5) \times 10^{-3}$

[a] For a plot, see Figure 3. [b] Average of three runs.

Table S3. Rate of reduction of PhCHO by ruthenium hydride **10** in toluene-d_8 at −64.4 ºC.

[**10**]$_0$ (M)	[PhCHO]$_0$ (M)	k_{obsd} (s^{-1}) [a]
0.0084	0.145	1.08(2) × 10^{-3}
0.0080	0.18	1.17(1) × 10^{-3}
0.0076	0.22	1.21(5) × 10^{-3}
0.0070	0.27	1.30(5) × 10^{-3}

[a] Average of three runs.

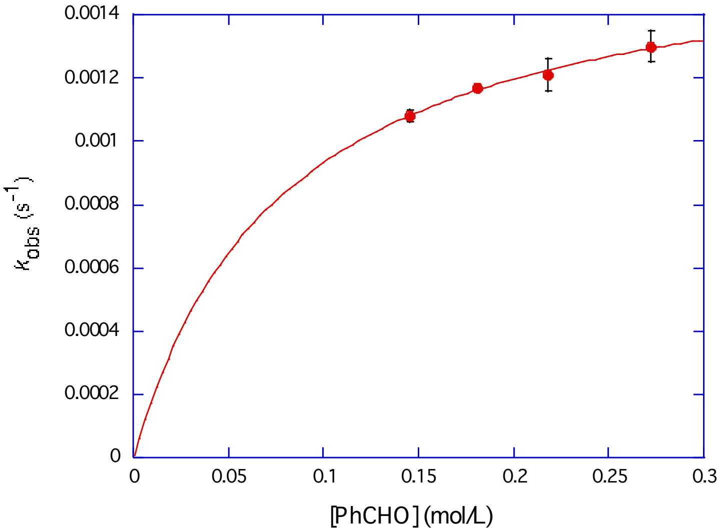

Figure S2. Plot of k_{obs} as a function of [PhCHO] in toluene-d_8 at −64.4 ºC.

$\Rightarrow K_{eq} = 12.6 \pm 1.5\ M^{-1}$ and $k_2 = 1.7 \pm 0.1 \times 10^{-3}\ s^{-1}$

Table S4. Rate of reduction of PhCHO by ruthenium hydride **10** in toluene-d_8 at −67.7 ºC.

[**10**]$_0$ (M)	[PhCHO]$_0$ (M)	k_{obsd} (s^{-1}) [a]
0.0084	0.145	$7.7(3) \times 10^{-4}$
0.0080	0.18	$8.2(1) \times 10^{-4}$
0.0076	0.22	$8.6(2) \times 10^{-4}$
0.0070	0.27	$9.1(4) \times 10^{-4}$

[a] Average of three runs.

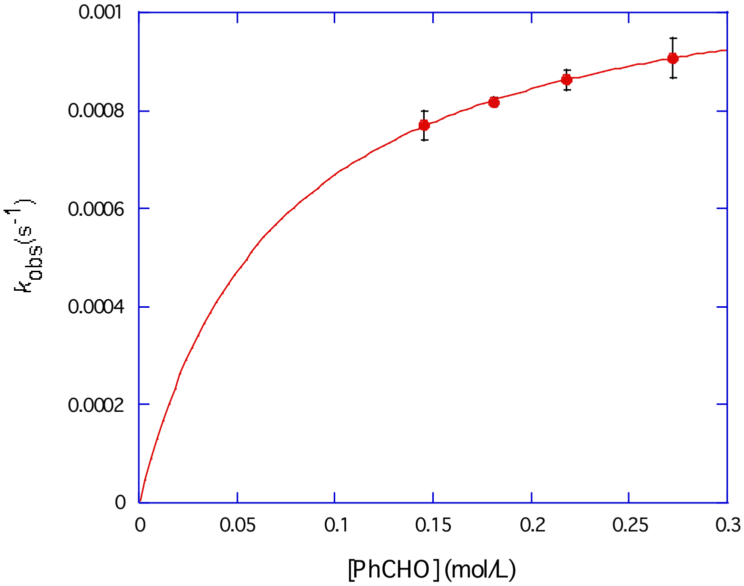

Figure S3. Plot of k_{obs} as a function of [PhCHO] in toluene-d_8 at −67.7 ºC.

$\Rightarrow K_{eq} = 14.1 \pm 0.6$ M^{-1} and $k_2 = 1.1 \pm 0.1 \times 10^{-3}$ s^{-1}

Table S5. Rate of Reduction of PhCHO by Ruthenium Hydride **10** in Toluene-d_8 at Various Temperatures.

T (K)	K_{eq} (M^{-1})	k_2 (s^{-1})	1/T (K^{-1})	$\ln(k_2/T)$	$\ln(K_{eq})$
219.6	3.6 ± 0.6	$1.0(1) \times 10^{-2}$	0.00455	−10.00(10)	1.28(17)
213.1	9.3 ± 1.1	$3.0(1) \times 10^{-3}$	0.00469	−11.17(3)	2.23(12)
208.7	12.6 ± 1.5	$1.7(1) \times 10^{-3}$	0.00479	−11.72(5)	2.53(12)
205.4	14.1 ± 0.6	$1.1(1) \times 10^{-3}$	0.00487	−12.14(9)	2.65(5)

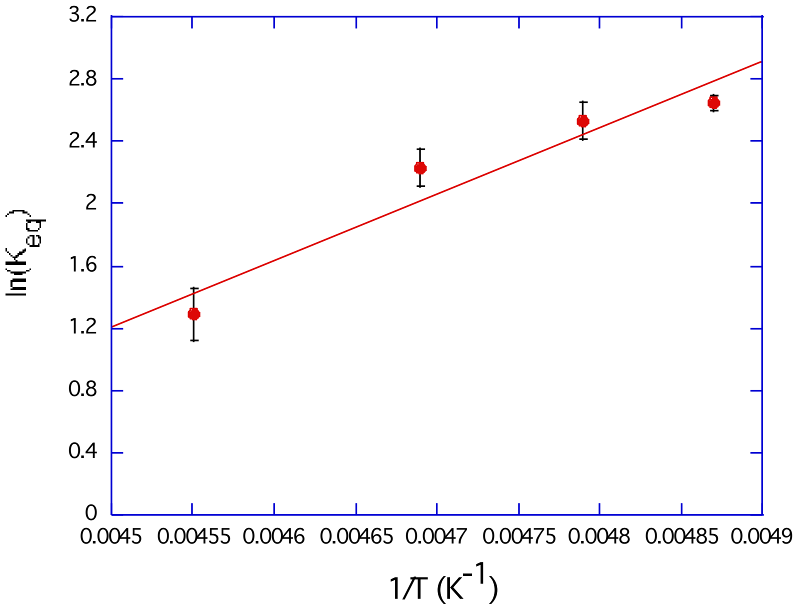

Figure S4. Van't Hoff Plot for Hydrogen Bonding Formation

$\Rightarrow \Delta H^\circ = -8.5 \pm 1.7$ kcal mol^{-1} and $\Delta S^\circ = -35.9 \pm 8.2$ eu

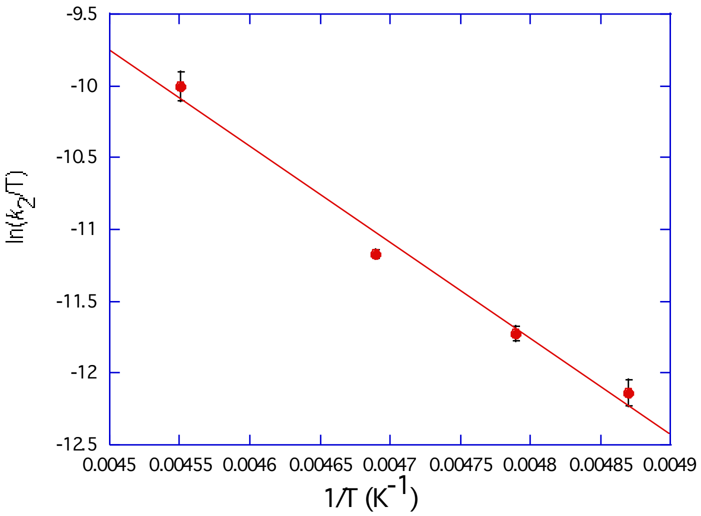

Figure S5. Eyring Plot for Hydrogen Transfer Step

⇒ $\Delta H^{\ddagger} = 13.3 \pm 1.3$ kcal mol^{-1} and $\Delta S^{\ddagger} = -6.7 \pm 6.2$ eu

[2,5-$(SiMe_3)_2$-3,4-(CH_2OCH_2)(η^5-C_4COD)]Ru$(CO)_2$D (10-*d*$_2$) was prepared in 63 % yield using a procedure that is similar to the synthesis of **10**, but employing 40 wt % of NaOD in D_2O and 85 wt % of D_3PO_4 in D_2O. The complex **10-*d*$_2$** was isolated with high isotopic purity (> 99 % deuterium at OD and 96 % deuterium at RuD).

^{2}H NMR Study of the Stoichiometric Reduction of Benzaldehyde by 10-*d*$_2$. A Teflon capped NMR tube containing a solution of **10-*d*$_2$** (12.8 mg, 30 μmol) in toluene (400 μL) was chilled in a dry ice/acetone bath, and a solution of PhCHO (30.5 μL, 300 μmol) in toluene (100 μL) was added via a gas tight syringe through the Teflon cap. The two solutions were carefully mixed while cold, and the NMR tube was immediately placed into a probe calibrated to -60 ºC. The progress of reduction was monitored by ^{2}H NMR spectroscopy. The first spectrum (which was taken 3 min after mixing) revealed a OD resonance at δ 7.8 (shifted from δ 4.7 in pure **10-**

***d*₂**). Even after 100 min, there was still some **10-*d*₂** left, suggesting that the reduction was significantly slower than the reduction with non-deuterated **10**.

NMR Measurements of Rate Constants for the Reduction of Acetophenone by Ruthenium and Iron Hydrides. The procedures were similar as PhCHO reduction, except that 2 equiv of PPh_3 was added as trapping agent and the reaction was monitored at 5.0 ºC. The results are summarized in Tables S6 and S7 and Figures S6 and S7.

Table S6. Rate of reduction of acetophenone by ruthenium hydride **10** in toluene-d_8 at 5.0 °C.

[**10**]$_0$ (M)	$[PhCOCH_3]_0$ (M)	$[PPh_3]_0$ (M)	k_{obsd} (s^{-1})
0.0090	0.10	0.018	$1.31(3) \times 10^{-3}$
0.0084	0.16	0.017	$1.86(4) \times 10^{-3}$
0.0080	0.20	0.016	$2.00(3) \times 10^{-3}$
0.0076	0.24	0.015	$2.12(3) \times 10^{-3}$

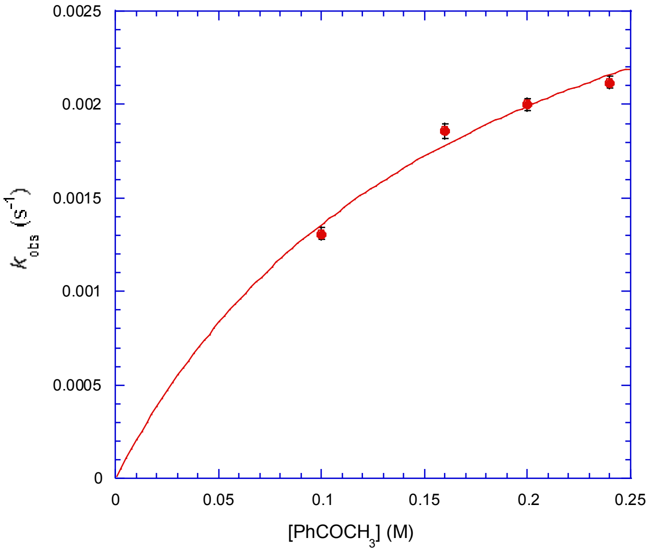

Figure S6. Plot of k_{obs} as a function of $[PhCOCH_3]$ in toluene-d_8 at 5.0 ºC.

$\Rightarrow K_{eq} = 5.7 \pm 1.6\ M^{-1}$ and $k_2 = 3.7 \pm 0.5 \times 10^{-3}\ s^{-1}$

Table S7. Rate of reduction of acetophenone by iron hydride **16** in toluene-d_8 at 5.0 °C.

[**16**]$_0$ (M)	[PhCOCH$_3$]$_0$ (M)	[PPh$_3$]$_0$ (M)	k_{obsd} (s^{-1})
0.0090	0.10	0.018	$9.2(7) \times 10^{-4}$
0.0084	0.16	0.017	$1.2(1) \times 10^{-3}$
0.0080	0.20	0.016	$1.4(1) \times 10^{-3}$
0.0076	0.24	0.015	$1.6(1) \times 10^{-3}$

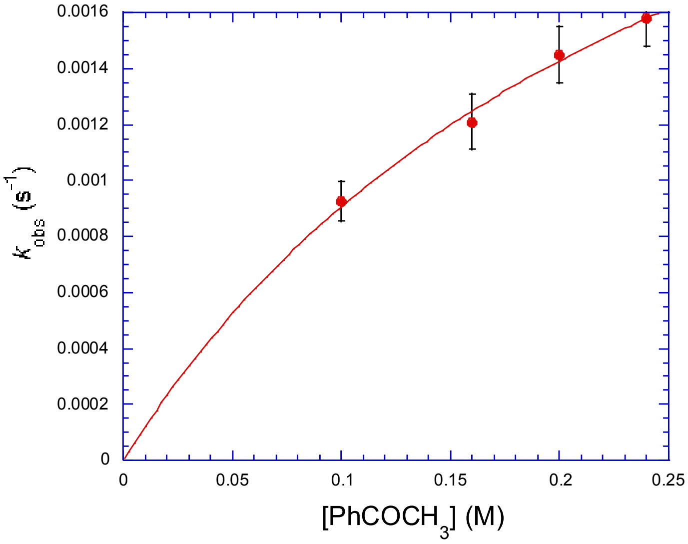

Figure S7. Plot of k_{obs} as a function of [PhCOCH$_3$] in toluene-d_8 at 5.0 ºC.

$\Rightarrow K_{eq} = 3.7 \pm 0.8$ M^{-1} and $k_2 = 3.4 \pm 0.3 \times 10^{-3}$ s^{-1}

Monitoring the Catalytic Hydrogenation of Acetophenone Catalyzed by 10. In a high-pressure vessel equipped with an attenuated total reflection IR detector, a solution of **10** in toluene was mixed with a solution of acetophenone in toluene at 25 °C under 35 atm of H_2 atmosphere. The IR spectra of the resulting reaction mixture were collected using an ASI Applied Systems ReactIR 1000 FTIR. The only ruthenium species observed during catalysis was **10** (2020 and 1960 cm^{-1}). The disappearance of acetophenone (at 1690 cm^{-1}) was monitored as a function of time.

Catalysis of the Hydrogenation of Carbonyls by 10 and 18. In a typical experiment, a carbonyl substrate (1.5 mmol) was added to a Fischer-Porter bottle under a nitrogen atmosphere. The bottle was flushed several times with hydrogen gas. Then, 5 mL of a solution of **10** (or **18**) in toluene (0.0060 M) was added by syringe under a flow of hydrogen and the resulting solution stirred under 3 atm of hydrogen at 25 °C. The progress the reaction was periodically monitored by analyzing the ^1H NMR spectra of aliquots withdrawn from the reaction mixture. When the hydrogenation was complete, hydrogenation products were purified by column chromatography and their ^1H NMR spectra matched those reported in the literature.

X-Ray Crystal Structure of [2,5-$(SiMe_3)_2$-3,4-(CH_2OCH_2)(η^5-C_4COH)]Ru$(CO)_2$H (10).

Data Collection. A colorless crystal with approximate dimensions 0.43 x 0.41 x 0.34 mm^3 was selected under oil under ambient conditions and attached to the tip of a nylon loop. The crystal was mounted in a stream of cold nitrogen at 100(2) K and centered in the X-ray beam by using a video camera. The crystal evaluation and data collection were performed on a Bruker CCD-1000 diffractometer with Mo K_α (λ = 0.71073 Å) radiation and the diffractometer to crystal distance of 4.9 cm. The initial cell constants were obtained from three series of ω scans at different starting angles. Each series consisted of 25 frames collected at intervals of 0.3° in a 6° range about ω with the exposure time of 10 seconds per frame. A total of 243 reflections was obtained. The reflections were successfully indexed by an automated indexing routine built in the SMART program. The final cell constants were calculated from a set of 27509 strong reflections from the actual data collection. The data were collected by using the full sphere data collection routine to survey the reciprocal space to the extent of a full sphere to a resolution of 0.80 Å. A total of 43015 data were harvested by collecting three sets of frames with 0.25° scans in ω and ϕ with an exposure time 15 sec per frame. These highly redundant datasets were corrected for Lorentz and polarization effects. The absorption correction was based on fitting a function to the empirical transmission surface as sampled by multiple equivalent measurements.[1]

Structure Solution and Refinement. The systematic absences in the diffraction data were uniquely consistent for the space group *Pbca* that yielded chemically reasonable and computationally stable results of refinement.[1] A successful solution by the direct methods provided most non-hydrogen atoms from the *E*-map. The remaining non-hydrogen atoms were located in an alternating series of least-squares cycles and difference Fourier maps. All non-hydrogen atoms were refined with anisotropic displacement coefficients. All hydrogen atoms except the hydride were included in the structure factor calculation at idealized positions and were allowed to ride on the neighboring atoms with relative isotropic displacement coefficients. The final least-squares refinement of 210 parameters against 4014 data resulted in residuals *R* (based on F^2 for $I \geq 2\sigma$) and *wR* (based on F^2 for all data) of 0.0167 and 0.0461, respectively. The final difference Fourier map was featureless. The ORTEP diagram is drawn with 50% probability ellipsoids.[i]

(1) Bruker-AXS. (2000-2003) SADABS V.2.05, SAINT V.6.22, SHELXTL V.6.10 & SMART 5.622 Software Reference Manuals. Bruker-AXS, Madison, Wisconsin, USA.

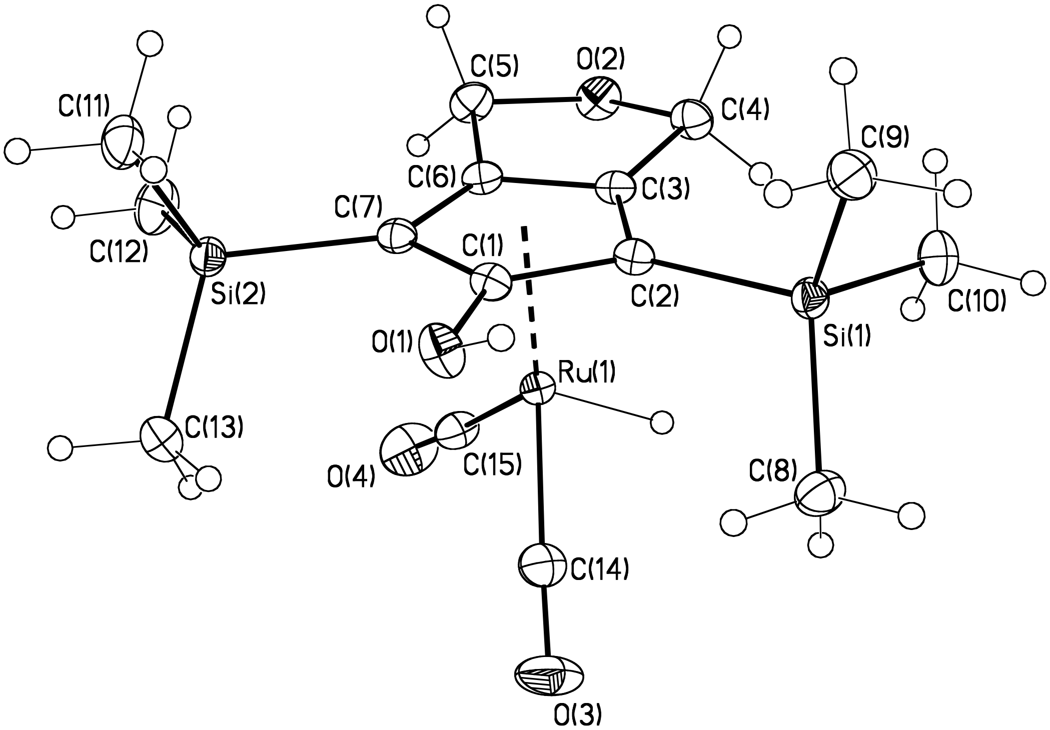

Table 1. Crystal data and structure refinement for [2,5-$(SiMe_3)_2$-3,4-(CH_2OCH_2)(η^5-C_4COH)]Ru$(CO)_2$H (**10**).

.

Empirical formula	$C_{15} H_{24} O_4 Ru Si_2$	
Formula weight	425.59	
Temperature	100(2) K	
Wavelength	0.71073 Å	
Crystal system	Orthorhombic	
Space group	Pbca	
Unit cell dimensions	a = 11.8861(5) Å	α= 90°.
	b = 15.2456(6) Å	β= 90°.
	c = 21.6070(8) Å	γ = 90°.
Volume	3915.4(3) $Å^3$	
Z	8	
Density (calculated)	1.444 Mg/m^3	
Absorption coefficient	0.935 mm^{-1}	
F(000)	1744	
Crystal size	0.43 x 0.41 x 0.34 mm^3	
Theta range for data collection	2.37 to 26.40°.	
Index ranges	-14<=h<=14, -19<=k<=19, -26<=l<=27	
Reflections collected	43015	
Independent reflections	4014 [R(int) = 0.0294]	
Completeness to theta = 26.40°	99.9 %	
Absorption correction	Multi-scan with SADABS	
Max. and min. transmission	0.7416 and 0.6892	
Refinement method	Full-matrix least-squares on F^2	
Data / restraints / parameters	4014 / 0 / 210	
Goodness-of-fit on F^2	1.004	
Final R indices [I>2sigma(I)]	R1 = 0.0167, wR2 = 0.0450	
R indices (all data)	R1 = 0.0181, wR2 = 0.0461	
Largest diff. peak and hole	0.378 and -0.245 e.$Å^{-3}$	

Table 2. Atomic coordinates (x 10^4) and equivalent isotropic displacement parameters (Å^{2}x 10^3) for [2,5-$(SiMe_3)_2$-3,4-(CH_2OCH_2)(η^5-C_4COH)]$Ru(CO)_2H$ (**10**). U(eq) is defined as one third of the trace of the orthogonalized U^{ij} tensor.

	x	y	z	U(eq)
Ru(1)	399(1)	195(1)	8822(1)	12(1)
Si(1)	2763(1)	1137(1)	9674(1)	15(1)
Si(2)	722(1)	724(1)	7167(1)	15(1)
O(1)	1614(1)	1936(1)	8279(1)	19(1)
O(2)	2047(1)	-1763(1)	8601(1)	21(1)
O(3)	-1049(1)	1649(1)	9339(1)	35(1)
O(4)	-1544(1)	-941(1)	8421(1)	34(1)
C(1)	1753(1)	1066(1)	8381(1)	14(1)
C(2)	2199(1)	651(1)	8936(1)	14(1)
C(3)	2164(1)	-271(1)	8782(1)	14(1)
C(4)	2549(1)	-1139(1)	9029(1)	19(1)
C(5)	1758(1)	-1340(1)	8018(1)	20(1)
C(6)	1689(1)	-389(1)	8194(1)	14(1)
C(7)	1400(1)	447(1)	7925(1)	14(1)
C(8)	1735(1)	1934(1)	10001(1)	21(1)
C(9)	4151(1)	1674(1)	9529(1)	21(1)
C(10)	2996(1)	210(1)	10222(1)	24(1)
C(11)	1777(1)	1284(1)	6668(1)	24(1)
C(12)	241(1)	-326(1)	6809(1)	27(1)
C(13)	-503(1)	1460(1)	7298(1)	26(1)
C(14)	-524(1)	1092(1)	9136(1)	21(1)
C(15)	-824(1)	-501(1)	8586(1)	21(1)

Table 3. Bond lengths [Å] and angles [°] for [2,5-(SiMe$_3$)$_2$-3,4-(CH$_2$OCH$_2$)(η^5-C$_4$COH)]Ru(CO)$_2$H (**10**).

Ru(1)-C(15)	1.8700(15)	C(3)-C(6)	1.4019(19)
Ru(1)-C(14)	1.8795(15)	C(3)-C(4)	1.4990(18)
Ru(1)-C(3)	2.2167(14)	C(4)-H(4A)	0.9900
Ru(1)-C(6)	2.2322(13)	C(4)-H(4B)	0.9900
Ru(1)-C(2)	2.2634(13)	C(5)-C(6)	1.5008(18)
Ru(1)-C(1)	2.2929(13)	C(5)-H(5A)	0.9900
Ru(1)-C(7)	2.3073(13)	C(5)-H(5B)	0.9900
Ru(1)-H(1)	1.55(2)	C(6)-C(7)	1.4421(18)
Ru(1)-Centroid	1.906(2)	C(8)-H(8A)	0.9800
Si(1)-C(8)	1.8631(15)	C(8)-H(8B)	0.9800
Si(1)-C(10)	1.8638(15)	C(8)-H(8C)	0.9800
Si(1)-C(9)	1.8676(14)	C(9)-H(9A)	0.9800
Si(1)-C(2)	1.8809(14)	C(9)-H(9B)	0.9800
Si(2)-C(13)	1.8598(15)	C(9)-H(9C)	0.9800
Si(2)-C(11)	1.8609(15)	C(10)-H(10A)	0.9800
Si(2)-C(12)	1.8684(16)	C(10)-H(10B)	0.9800
Si(2)-C(7)	1.8726(14)	C(10)-H(10C)	0.9800
O(1)-C(1)	1.3545(16)	C(11)-H(11A)	0.9800
O(1)-H(1A)	0.8400	C(11)-H(11B)	0.9800
O(2)-C(5)	1.4548(17)	C(11)-H(11C)	0.9800
O(2)-C(4)	1.4544(17)	C(12)-H(12A)	0.9800
O(3)-C(14)	1.1412(18)	C(12)-H(12B)	0.9800
O(4)-C(15)	1.1445(19)	C(12)-H(12C)	0.9800
C(1)-C(7)	1.4283(18)	C(13)-H(13A)	0.9800
C(1)-C(2)	1.4559(18)	C(13)-H(13B)	0.9800
C(2)-C(3)	1.4451(19)	C(13)-H(13C)	0.9800

C(15)-Ru(1)-C(14)	93.31(6)	C(14)-Ru(1)-C(7)	118.96(6)
C(15)-Ru(1)-C(3)	122.89(6)	C(3)-Ru(1)-C(7)	62.12(5)
C(14)-Ru(1)-C(3)	143.06(5)	C(6)-Ru(1)-C(7)	37.00(5)
C(15)-Ru(1)-C(6)	98.15(6)	C(2)-Ru(1)-C(7)	63.45(5)
C(14)-Ru(1)-C(6)	155.58(6)	C(1)-Ru(1)-C(7)	36.18(5)
C(3)-Ru(1)-C(6)	36.73(5)	C(15)-Ru(1)-H(1)	85.5(8)
C(15)-Ru(1)-C(2)	159.82(6)	C(14)-Ru(1)-H(1)	85.3(8)
C(14)-Ru(1)-C(2)	106.78(5)	C(3)-Ru(1)-H(1)	90.1(8)
C(3)-Ru(1)-C(2)	37.62(5)	C(6)-Ru(1)-H(1)	116.9(8)
C(6)-Ru(1)-C(2)	62.58(5)	C(2)-Ru(1)-H(1)	97.7(8)
C(15)-Ru(1)-C(1)	139.51(6)	C(1)-Ru(1)-H(1)	134.0(8)
C(14)-Ru(1)-C(1)	97.97(6)	C(7)-Ru(1)-H(1)	151.9(8)
C(3)-Ru(1)-C(1)	60.35(5)	C(8)-Si(1)-C(10)	110.53(7)
C(6)-Ru(1)-C(1)	59.77(5)	C(8)-Si(1)-C(9)	110.93(7)
C(2)-Ru(1)-C(1)	37.26(5)	C(10)-Si(1)-C(9)	107.90(7)
C(15)-Ru(1)-C(7)	105.43(5)	C(8)-Si(1)-C(2)	110.15(6)

C(10)-Si(1)-C(2)	107.02(6)
C(9)-Si(1)-C(2)	110.20(6)
C(13)-Si(2)-C(11)	109.82(7)
C(13)-Si(2)-C(12)	109.94(8)
C(11)-Si(2)-C(12)	110.99(7)
C(13)-Si(2)-C(7)	109.92(6)
C(11)-Si(2)-C(7)	108.65(6)
C(12)-Si(2)-C(7)	107.48(7)
C(1)-O(1)-H(1A)	109.5
C(5)-O(2)-C(4)	110.93(10)
O(1)-C(1)-C(7)	119.91(12)
O(1)-C(1)-C(2)	127.15(12)
C(7)-C(1)-C(2)	112.90(11)
O(1)-C(1)-Ru(1)	123.33(9)
C(7)-C(1)-Ru(1)	72.46(7)
C(2)-C(1)-Ru(1)	70.27(7)
C(3)-C(2)-C(1)	102.82(11)
C(3)-C(2)-Si(1)	126.02(10)
C(1)-C(2)-Si(1)	131.10(10)
C(3)-C(2)-Ru(1)	69.44(7)
C(1)-C(2)-Ru(1)	72.47(7)
Si(1)-C(2)-Ru(1)	123.39(6)
C(6)-C(3)-C(2)	110.20(12)
C(6)-C(3)-C(4)	109.36(12)
C(2)-C(3)-C(4)	140.24(13)
C(6)-C(3)-Ru(1)	72.24(8)
C(2)-C(3)-Ru(1)	72.95(7)
C(4)-C(3)-Ru(1)	123.95(9)
O(2)-C(4)-C(3)	103.05(11)
O(2)-C(4)-H(4A)	111.2
C(3)-C(4)-H(4A)	111.2
O(2)-C(4)-H(4B)	111.2
C(3)-C(4)-H(4B)	111.2
H(4A)-C(4)-H(4B)	109.1
O(2)-C(5)-C(6)	102.82(11)
O(2)-C(5)-H(5A)	111.2
C(6)-C(5)-H(5A)	111.2
O(2)-C(5)-H(5B)	111.2
C(6)-C(5)-H(5B)	111.2
H(5A)-C(5)-H(5B)	109.1
C(3)-C(6)-C(7)	110.40(12)
C(3)-C(6)-C(5)	109.37(12)
C(7)-C(6)-C(5)	139.79(12)
C(3)-C(6)-Ru(1)	71.03(8)
C(7)-C(6)-Ru(1)	74.33(7)
C(5)-C(6)-Ru(1)	125.21(9)
C(1)-C(7)-C(6)	103.58(11)
C(1)-C(7)-Si(2)	125.48(10)
C(6)-C(7)-Si(2)	130.94(10)
C(1)-C(7)-Ru(1)	71.36(7)
C(6)-C(7)-Ru(1)	68.67(7)
Si(2)-C(7)-Ru(1)	123.33(6)
Si(1)-C(8)-H(8A)	109.5
Si(1)-C(8)-H(8B)	109.5
H(8A)-C(8)-H(8B)	109.5
Si(1)-C(8)-H(8C)	109.5
H(8A)-C(8)-H(8C)	109.5
H(8B)-C(8)-H(8C)	109.5
Si(1)-C(9)-H(9A)	109.5
Si(1)-C(9)-H(9B)	109.5
H(9A)-C(9)-H(9B)	109.5
Si(1)-C(9)-H(9C)	109.5
H(9A)-C(9)-H(9C)	109.5
H(9B)-C(9)-H(9C)	109.5
Si(1)-C(10)-H(10A)	109.5
Si(1)-C(10)-H(10B)	109.5
H(10A)-C(10)-H(10B)	109.5
Si(1)-C(10)-H(10C)	109.5
H(10A)-C(10)-H(10C)	109.5
H(10B)-C(10)-H(10C)	109.5
Si(2)-C(11)-H(11A)	109.5
Si(2)-C(11)-H(11B)	109.5
H(11A)-C(11)-H(11B)	109.5
Si(2)-C(11)-H(11C)	109.5
H(11A)-C(11)-H(11C)	109.5
H(11B)-C(11)-H(11C)	109.5
Si(2)-C(12)-H(12A)	109.5
Si(2)-C(12)-H(12B)	109.5
H(12A)-C(12)-H(12B)	109.5
Si(2)-C(12)-H(12C)	109.5
H(12A)-C(12)-H(12C)	109.5
H(12B)-C(12)-H(12C)	109.5
Si(2)-C(13)-H(13A)	109.5
Si(2)-C(13)-H(13B)	109.5
H(13A)-C(13)-H(13B)	109.5
Si(2)-C(13)-H(13C)	109.5
H(13A)-C(13)-H(13C)	109.5
H(13B)-C(13)-H(13C)	109.5
O(3)-C(14)-Ru(1)	177.37(13)
O(4)-C(15)-Ru(1)	177.06(13)

Table 4. Anisotropic displacement parameters (Å^{2}x 10^3) for [2,5-(SiMe$_3$)$_2$-3,4-(CH$_2$OCH$_2$)(η^5-C$_4$COH)]Ru(CO)$_2$H (**10**). The anisotropic displacement factor exponent takes the form: $-2\pi^2[\,h^2 a^{*2}U^{11} + ... + 2\,h\,k\,a^*\,b^*\,U^{12}\,]$

	U^{11}	U^{22}	U^{33}	U^{23}	U^{13}	U^{12}
Ru(1)	12(1)	11(1)	13(1)	-1(1)	1(1)	-1(1)
Si(1)	14(1)	17(1)	14(1)	-1(1)	-1(1)	-1(1)
Si(2)	14(1)	18(1)	13(1)	1(1)	-1(1)	-1(1)
O(1)	23(1)	10(1)	24(1)	2(1)	-7(1)	-2(1)
O(2)	29(1)	10(1)	23(1)	1(1)	2(1)	2(1)
O(3)	22(1)	34(1)	49(1)	-23(1)	-3(1)	7(1)
O(4)	26(1)	36(1)	40(1)	-11(1)	1(1)	-14(1)
C(1)	13(1)	13(1)	17(1)	2(1)	1(1)	-1(1)
C(2)	13(1)	11(1)	16(1)	0(1)	1(1)	0(1)
C(3)	13(1)	12(1)	17(1)	1(1)	3(1)	1(1)
C(4)	20(1)	14(1)	21(1)	2(1)	0(1)	3(1)
C(5)	25(1)	13(1)	20(1)	-1(1)	2(1)	2(1)
C(6)	14(1)	13(1)	17(1)	-1(1)	3(1)	0(1)
C(7)	13(1)	14(1)	15(1)	1(1)	2(1)	0(1)
C(8)	20(1)	23(1)	21(1)	-5(1)	2(1)	-1(1)
C(9)	17(1)	25(1)	22(1)	-3(1)	-1(1)	-4(1)
C(10)	28(1)	27(1)	18(1)	4(1)	-4(1)	0(1)
C(11)	21(1)	32(1)	18(1)	6(1)	-1(1)	-4(1)
C(12)	32(1)	28(1)	21(1)	-3(1)	-4(1)	-8(1)
C(13)	22(1)	36(1)	21(1)	3(1)	-2(1)	9(1)
C(14)	15(1)	23(1)	25(1)	-6(1)	-2(1)	-3(1)
C(15)	19(1)	22(1)	21(1)	-3(1)	4(1)	-1(1)

Table 5. Hydrogen coordinates (x 10^4) and isotropic displacement parameters (Å^{2}x 10^3) for [2,5-$(SiMe_3)_2$-3,4-(CH_2OCH_2)(η^5-C_4COH)]$Ru(CO)_2H$ (**10**).

	x	y	z	U(eq)
H(1)	257(18)	-235(14)	9469(11)	50(7)
H(1A)	2111	2217	8471	28
H(4A)	3380	-1183	9025	22
H(4B)	2274	-1235	9456	22
H(5A)	1028	-1555	7858	23
H(5B)	2347	-1439	7702	23
H(8A)	2089	2262	10339	32
H(8B)	1078	1616	10160	32
H(8C)	1495	2342	9677	32
H(9A)	4459	1891	9921	31
H(9B)	4050	2165	9243	31
H(9C)	4672	1246	9348	31
H(10A)	3572	-184	10054	37
H(10B)	2291	-114	10277	37
H(10C)	3246	441	10622	37
H(11A)	1436	1423	6267	35
H(11B)	2425	896	6605	35
H(11C)	2025	1826	6869	35
H(12A)	-289	-620	7087	40
H(12B)	892	-708	6737	40
H(12C)	-131	-202	6414	40
H(13A)	-1113	1129	7494	39
H(13B)	-763	1695	6901	39
H(13C)	-279	1946	7569	39

Table 6. Torsion angles [°] for [2,5-(SiMe$_3$)$_2$-3,4-(CH$_2$OCH$_2$)(η^5-C$_4$COH)]Ru(CO)$_2$H (**10**).

H(1)-Ru(1)-C(1)-O(1)	-106.0(1.1)	C(15)-Ru(1)-C(2)-Si(1)	-138.16(15)
C(15)-Ru(1)-C(1)-O(1)	89.88(13)	C(14)-Ru(1)-C(2)-Si(1)	47.17(9)
C(14)-Ru(1)-C(1)-O(1)	-14.83(12)	C(3)-Ru(1)-C(2)-Si(1)	-120.33(12)
C(3)-Ru(1)-C(1)-O(1)	-162.93(13)	C(6)-Ru(1)-C(2)-Si(1)	-156.63(9)
C(6)-Ru(1)-C(1)-O(1)	154.43(13)	C(1)-Ru(1)-C(2)-Si(1)	128.13(12)
C(2)-Ru(1)-C(1)-O(1)	-122.14(14)	C(7)-Ru(1)-C(2)-Si(1)	161.67(9)
C(7)-Ru(1)-C(1)-O(1)	114.71(14)	C(1)-C(2)-C(3)-C(6)	-2.39(14)
C(15)-Ru(1)-C(1)-C(7)	-24.83(12)	Si(1)-C(2)-C(3)-C(6)	-179.93(10)
C(14)-Ru(1)-C(1)-C(7)	-129.54(8)	Ru(1)-C(2)-C(3)-C(6)	63.07(10)
C(3)-Ru(1)-C(1)-C(7)	82.36(8)	C(1)-C(2)-C(3)-C(4)	171.54(17)
C(6)-Ru(1)-C(1)-C(7)	39.72(7)	Si(1)-C(2)-C(3)-C(4)	-6.0(2)
C(2)-Ru(1)-C(1)-C(7)	123.15(11)	Ru(1)-C(2)-C(3)-C(4)	-123.00(19)
C(15)-Ru(1)-C(1)-C(2)	-147.98(9)	C(1)-C(2)-C(3)-Ru(1)	-65.46(8)
C(14)-Ru(1)-C(1)-C(2)	107.31(8)	Si(1)-C(2)-C(3)-Ru(1)	117.00(10)
C(3)-Ru(1)-C(1)-C(2)	-40.79(7)	C(15)-Ru(1)-C(3)-C(6)	54.25(10)
C(6)-Ru(1)-C(1)-C(2)	-83.43(8)	C(14)-Ru(1)-C(3)-C(6)	-138.69(10)
C(7)-Ru(1)-C(1)-C(2)	-123.15(11)	C(2)-Ru(1)-C(3)-C(6)	-118.53(11)
O(1)-C(1)-C(2)-C(3)	-179.29(13)	C(1)-Ru(1)-C(3)-C(6)	-78.13(8)
C(7)-C(1)-C(2)-C(3)	3.21(14)	C(7)-Ru(1)-C(3)-C(6)	-36.69(7)
Ru(1)-C(1)-C(2)-C(3)	63.28(8)	C(15)-Ru(1)-C(3)-C(2)	172.78(8)
O(1)-C(1)-C(2)-Si(1)	-1.9(2)	C(14)-Ru(1)-C(3)-C(2)	-20.16(13)
C(7)-C(1)-C(2)-Si(1)	-179.43(10)	C(6)-Ru(1)-C(3)-C(2)	118.53(11)
Ru(1)-C(1)-C(2)-Si(1)	-119.36(11)	C(1)-Ru(1)-C(3)-C(2)	40.40(7)
O(1)-C(1)-C(2)-Ru(1)	117.43(13)	C(7)-Ru(1)-C(3)-C(2)	81.84(8)
C(7)-C(1)-C(2)-Ru(1)	-60.07(10)	C(15)-Ru(1)-C(3)-C(4)	-47.51(13)
C(8)-Si(1)-C(2)-C(3)	-131.22(12)	C(14)-Ru(1)-C(3)-C(4)	119.55(13)
C(10)-Si(1)-C(2)-C(3)	-11.02(13)	C(6)-Ru(1)-C(3)-C(4)	-101.76(14)
C(9)-Si(1)-C(2)-C(3)	106.06(12)	C(2)-Ru(1)-C(3)-C(4)	139.71(15)
C(8)-Si(1)-C(2)-C(1)	51.96(14)	C(1)-Ru(1)-C(3)-C(4)	-179.89(13)
C(10)-Si(1)-C(2)-C(1)	172.16(12)	C(7)-Ru(1)-C(3)-C(4)	-138.45(12)
C(9)-Si(1)-C(2)-C(1)	-70.76(14)	C(5)-O(2)-C(4)-C(3)	20.62(14)
C(8)-Si(1)-C(2)-Ru(1)	-43.56(9)	C(6)-C(3)-C(4)-O(2)	-11.53(14)
C(10)-Si(1)-C(2)-Ru(1)	76.64(9)	C(2)-C(3)-C(4)-O(2)	174.51(16)
C(9)-Si(1)-C(2)-Ru(1)	-166.28(7)	Ru(1)-C(3)-C(4)-O(2)	69.65(13)
C(15)-Ru(1)-C(2)-C(3)	-17.8(2)	C(4)-O(2)-C(5)-C(6)	-21.21(14)
C(14)-Ru(1)-C(2)-C(3)	167.51(8)	C(2)-C(3)-C(6)-C(7)	0.86(16)
C(6)-Ru(1)-C(2)-C(3)	-36.30(7)	C(4)-C(3)-C(6)-C(7)	-175.03(11)
C(1)-Ru(1)-C(2)-C(3)	-111.54(11)	Ru(1)-C(3)-C(6)-C(7)	64.37(9)
C(7)-Ru(1)-C(2)-C(3)	-78.00(8)	C(2)-C(3)-C(6)-C(5)	174.79(11)
C(15)-Ru(1)-C(2)-C(1)	93.71(17)	C(4)-C(3)-C(6)-C(5)	-1.10(16)
C(14)-Ru(1)-C(2)-C(1)	-80.96(9)	Ru(1)-C(3)-C(6)-C(5)	-121.70(10)
C(3)-Ru(1)-C(2)-C(1)	111.54(11)	C(2)-C(3)-C(6)-Ru(1)	-63.51(9)
C(6)-Ru(1)-C(2)-C(1)	75.24(8)	C(4)-C(3)-C(6)-Ru(1)	120.60(11)
C(7)-Ru(1)-C(2)-C(1)	33.54(7)	O(2)-C(5)-C(6)-C(3)	13.24(15)

O(2)-C(5)-C(6)-C(7)	-175.59(15)
O(2)-C(5)-C(6)-Ru(1)	-66.76(14)
C(15)-Ru(1)-C(6)-C(3)	-136.50(8)
C(14)-Ru(1)-C(6)-C(3)	106.33(14)
C(2)-Ru(1)-C(6)-C(3)	37.17(8)
C(1)-Ru(1)-C(6)-C(3)	79.82(8)
C(7)-Ru(1)-C(6)-C(3)	118.63(11)
C(15)-Ru(1)-C(6)-C(7)	104.87(8)
C(14)-Ru(1)-C(6)-C(7)	-12.30(17)
C(3)-Ru(1)-C(6)-C(7)	-118.63(11)
C(2)-Ru(1)-C(6)-C(7)	-81.47(8)
C(1)-Ru(1)-C(6)-C(7)	-38.81(7)
C(15)-Ru(1)-C(6)-C(5)	-35.73(12)
C(14)-Ru(1)-C(6)-C(5)	-152.91(13)
C(3)-Ru(1)-C(6)-C(5)	100.76(14)
C(2)-Ru(1)-C(6)-C(5)	137.93(13)
C(1)-Ru(1)-C(6)-C(5)	-179.42(13)
C(7)-Ru(1)-C(6)-C(5)	-140.60(15)
O(1)-C(1)-C(7)-C(6)	179.57(11)
C(2)-C(1)-C(7)-C(6)	-2.74(15)
Ru(1)-C(1)-C(7)-C(6)	-61.55(8)
O(1)-C(1)-C(7)-Si(2)	-0.74(18)
C(2)-C(1)-C(7)-Si(2)	176.96(9)
Ru(1)-C(1)-C(7)-Si(2)	118.15(10)
O(1)-C(1)-C(7)-Ru(1)	-118.88(12)
C(2)-C(1)-C(7)-Ru(1)	58.81(9)
C(3)-C(6)-C(7)-C(1)	1.11(15)
C(5)-C(6)-C(7)-C(1)	-170.00(16)
Ru(1)-C(6)-C(7)-C(1)	63.43(9)
C(3)-C(6)-C(7)-Si(2)	-178.57(10)
C(5)-C(6)-C(7)-Si(2)	10.3(3)
Ru(1)-C(6)-C(7)-Si(2)	-116.24(11)
C(3)-C(6)-C(7)-Ru(1)	-62.32(9)
C(5)-C(6)-C(7)-Ru(1)	126.57(18)
C(13)-Si(2)-C(7)-C(1)	-51.91(13)
C(11)-Si(2)-C(7)-C(1)	68.29(13)
C(12)-Si(2)-C(7)-C(1)	-171.54(11)
C(13)-Si(2)-C(7)-C(6)	127.70(13)
C(11)-Si(2)-C(7)-C(6)	-112.10(13)
C(12)-Si(2)-C(7)-C(6)	8.07(15)
C(13)-Si(2)-C(7)-Ru(1)	38.04(10)
C(11)-Si(2)-C(7)-Ru(1)	158.23(7)
C(12)-Si(2)-C(7)-Ru(1)	-81.60(9)
C(15)-Ru(1)-C(7)-C(1)	163.57(8)
C(14)-Ru(1)-C(7)-C(1)	60.78(9)
C(3)-Ru(1)-C(7)-C(1)	-77.01(8)
C(6)-Ru(1)-C(7)-C(1)	-113.44(11)
C(2)-Ru(1)-C(7)-C(1)	-34.52(7)
C(15)-Ru(1)-C(7)-C(6)	-82.99(9)
C(14)-Ru(1)-C(7)-C(6)	174.22(8)
C(3)-Ru(1)-C(7)-C(6)	36.43(8)
C(2)-Ru(1)-C(7)-C(6)	78.92(8)
C(1)-Ru(1)-C(7)-C(6)	113.44(11)
C(15)-Ru(1)-C(7)-Si(2)	42.81(9)
C(14)-Ru(1)-C(7)-Si(2)	-59.97(9)
C(3)-Ru(1)-C(7)-Si(2)	162.24(9)
C(6)-Ru(1)-C(7)-Si(2)	125.81(12)
C(2)-Ru(1)-C(7)-Si(2)	-155.27(9)
C(1)-Ru(1)-C(7)-Si(2)	-120.75(11)
C(15)-Ru(1)-C(14)-O(3)	164(3)
C(3)-Ru(1)-C(14)-O(3)	-5(3)
C(6)-Ru(1)-C(14)-O(3)	-78(3)
C(2)-Ru(1)-C(14)-O(3)	-18(3)
C(1)-Ru(1)-C(14)-O(3)	-55(3)
C(7)-Ru(1)-C(14)-O(3)	-86(3)
C(14)-Ru(1)-C(15)-O(4)	149(3)
C(3)-Ru(1)-C(15)-O(4)	-38(3)
C(6)-Ru(1)-C(15)-O(4)	-9(3)
C(2)-Ru(1)-C(15)-O(4)	-25(3)
C(1)-Ru(1)-C(15)-O(4)	43(3)
C(7)-Ru(1)-C(15)-O(4)	28(3)

Table 7. Hydrogen bonds for [2,5-$(SiMe_3)_2$-3,4-(CH_2OCH_2)(η^5-C_4COH)]Ru$(CO)_2$H (**10**). [Å and °].

D-H...A	d(D-H)	d(H...A)	d(D...A)	<(DHA)
O(1)-H(1A)...O(2)#1	0.84	1.87	2.6373(13)	151.0

Symmetry transformations used to generate equivalent atoms:
#1 -x+1/2,y+1/2,z